



Proceedings of the Twelfth International Conference on
Engineering Computational Technology
Edited by: P. Iványi, J. Kruis and B.H.V. Topping
Civil-Comp Conferences, Volume 8, Paper 3.2
Civil-Comp Press, Edinburgh, United Kingdom, 2024
ISSN: 2753-3239, doi: 10.4203/ccc.8.3.2
©Civil-Comp Ltd, Edinburgh, UK, 2024

Investigating the Combined Effects of Temperature and Humidity on the Dynamic Properties of Concrete Beams

**M. Chaabi, A. Lampropoulos, O. Tsioulou
and P. Cacciola**

**School of Architecture, Technology and Engineering, University
of Brighton, United Kingdom**

Abstract

The dynamic response of structures can be significantly affected by environmental actions. Changes in natural frequencies and damping ratio due to the variation of temperature and humidity is widely recognized but not yet fully understood. Moreover, the performance of various passive control systems and the reliability of structural health monitoring systems can significantly be altered by the lack of understanding of the influence of hygrothermal actions on the dynamic response. In this paper modal hammer tests have been conducted on concrete beams with different strengths in a controlled environmental chamber for various temperatures and a constant range of relative humidity. The results showed that the first three frequencies decreased, as the temperature increased from -10°C to 30°C . The results of an optimization algorithm also were used to extract the dynamic modulus of elasticity and the loss factor. While the former showed a drop, the latter increased for the same range of temperature. Interestingly, different mix designs have manifested different sensitivity to thermal changes.

Keywords: modal test, natural frequencies, concrete beams, temperature, humidity, environmental chamber.

1 Introduction

Influence of temperature and humidity on the eigenproperties of structural elements has been highlighted in the literature in the past four decades (e.g.[1][2][3]). Correlation between temperature, humidity and natural frequencies of a concrete slab

was examined in a previous study, showing a negative correlation between temperature and natural frequencies [2], i.e. an increment of temperature/humidity leads to a reduction of the values of the natural frequencies. The findings from measurements of a nine-story reinforced concrete building [4] confirmed the same correlation between temperature and natural frequencies. The dynamic response of several other real-size concrete buildings and bridges has also been studied to evaluate the effect of ambient temperature and humidity on dynamic properties of these structures [5][6]. In a study by Liu and Wolf 2007 [6] the results from the study of a curved posttensioned concrete bridge under ambient loads, showed a linear negative relationship between temperature and first three natural frequencies. The vast majority of published studies in this field are based on in-situ measurements of frequency and damping under different temperatures and humidities, considering their daily and seasonally cyclic fluctuations (e.g. [7]), and there are very limited experimental studies of such structures in a controlled environment [8][9]. Field measurements are affected by additional environmental factors (such as wind [10][11], and rainfall [12]), and in-service conditions [11][13], hindering an accurate evaluation, and therefore preventing understanding, of the individual correlations. Therefore, to accurately quantify the effects of temperature and humidity on structural modal properties, it is crucial to minimize or even eliminate the effect of other external factors.

Although the influence of environmental factors on the dynamic response of structures is widely recognized, there is a lack of understanding of the inherent mechanism how the hygrothermal actions affect the dynamic properties of structures and the consequent dynamic response. The thorough understanding of the phenomenon is of paramount importance for structures exposed to large variability of environmental conditions and for the threads imposed by Climate Change.

This study is focused on concrete elements which have been found to be particularly sensitive to hygrothermal actions[14]. Modal testing on concrete beams in an environmental chamber with controlled temperature and relative humidity are undertaken in this study. Two different concrete strengths are used, and trends of the variation of natural frequencies and damping ratio are examined. The influence of the mix design (and pertinent compressive strengths) on the hygrothermal sensitivity of the modal properties is highlighted.

2 Methods

To investigate the effect of temperature on the eigenproperties of concrete beams, four beams and six cubes were cast using two different mix designs. One beam of each strength was put in the Environmental Chamber for dynamic tests, and the rest of the samples were used to identify the compressive strength of the mix design and the static young modulus of the beams.

2.1 Mix Design

Two different mix designs of Ordinary Portland Cement (OPC) concrete, were used, as presented in Table 1.

| Constituents | Mix 1 | Mix 2 |
|--------------------------------|-------|-------|
| Cement [kg/m ³] | 415 | 630 |
| Water [kg/m ³] | 220 | 220 |
| Sand [kg/m ³] | 530 | 465 |
| Aggregates[kg/m ³] | 1235 | 1085 |

Table1: Concrete Mix designs.

Compressive strength of the mixes was tested 28 days after casting using 100mm cubes, in accordance with BS 1881-116:1983 Standards[15]. The compressive testing machine illustrated in Figure 1 was utilized to provide the maximum load output in kN.



Figure 1: Compressive test of the cubes.

Results for the compressive strength of the mixes are given in Table 2.

| Specimen No. | Mix 1 strength [MPa] | Mix 2 strength [MPa] |
|--------------|----------------------|----------------------|
| Specimen 1 | 44.56 | 62.59 |
| Specimen 2 | 45.56 | 67.67 |
| Specimen 3 | 51.64 | 60.64 |
| Average | 47.25 | 63.63 |

Table 2: Compressive test results

2.2 Concrete beams

Using the mix designs presented above, four concrete beams (two per mix) were cast. Dimensions of the beams were 100mm x 55mm x 1000mm. During casting, three small holes of 2.75 cm depth and 3 mm diameter, were created in the beams for the three thermocouples which were embedded in the beams to measure the internal temperature. After that, the specimens were vibrated to ensure full contact of the thermocouples with the concrete. Then the beams were covered with plastic sheets for two days, and after demoulding, they were placed in a water tank for 28 days. After that period, specimens were stored under room conditions for one month, before starting the modal testing.



Figure 2: concrete beam with three embedded thermocouples.

Three-point bending tests have been then conducted on two beams (one for each mix design), and Linear Variable Differential Transformers (LVDTs) were used to measure the mid-span displacement. The load-mid span displacement results are illustrated in the Figure 3 showing the different strength of the materials and their similar modulus of elasticity.

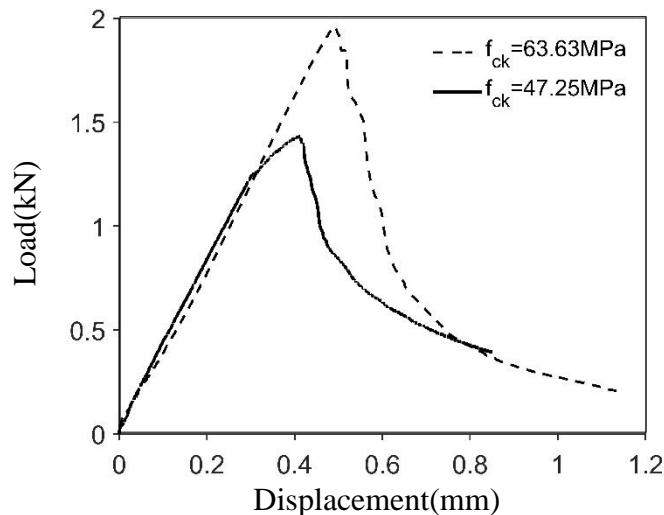


Figure 3: Three-point bending test results of the beams with compressive strength of 63.63MPa and 47.25MPa.

2.3 Modal Testing and structural identification

In this study, several impact-hammer tests were performed in an environmental chamber (4.2m×5.2m×4m, able to control room temperature ranging between -40°C to +60°C and humidity up to 70% relative humidity (RH) at 20°C), for dynamic identification of the concrete beams under different temperatures.

A free-free boundary condition was implemented by suspending the beam from a frame using two steel cords. The suspensions were placed at 2.5 cm distance from the edges of the beam (Figure 4). To ensure the minimum interference by the suspension on the lowest bending mode, the highest rigid body mode frequency was checked to be less than 20% of that of the first bending mode. This criterion would ensure preventing any significant influence of the test set-up on the flexural modes [16].

The 333B30 model PCB accelerometers then were attached to the beam on 25, 50, and 75 cm distances from one edge of the beam, as shown below in Figure 4. These accelerometers are capable of performing reliably in temperature range of -18 to +66°C. Modal hammer test have been then conducted using LMS-Siemens Scadas mobile acquisition system for joint measurement of temperature and vibrations. The results for the three measurement points have stored in the vectors $\mathbf{H}_i^{\text{measured}}(f)$ ($i=1,2,3$) with f indicating the frequency in Hz.

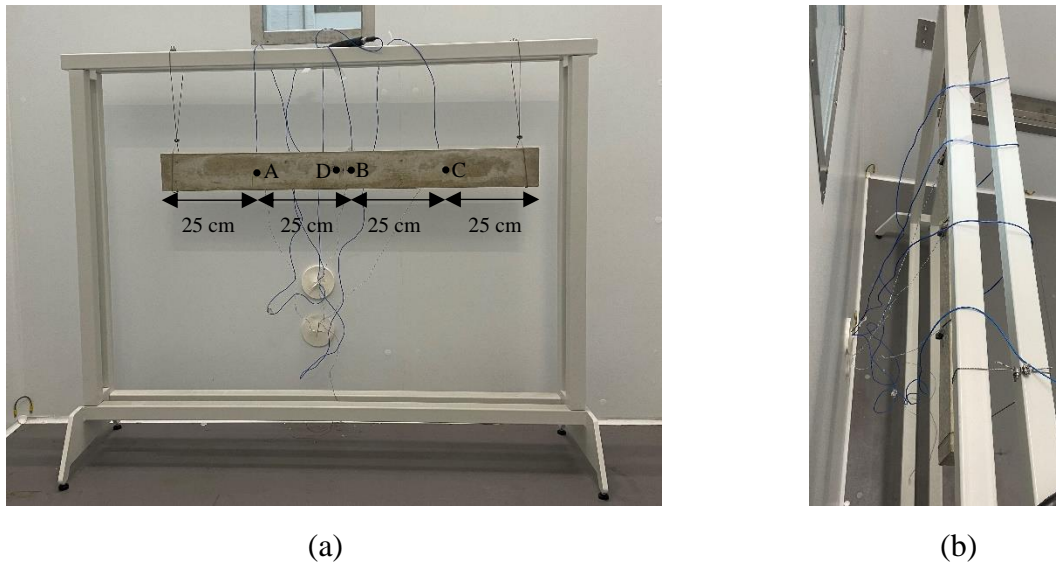


Figure 4: a) Front view of test setup, and A, B, and C, position of accelerometers, and D, hitting point at 2.5 cm from the centre of the beam. b) top view of test setup.

To determine the dynamic properties of the test specimens a structural identification approach in the frequency domain has been performed. To this aim a numerical model of the beam: forty 2D beam elements, two nodes, and two degrees

of freedom per node (one translational and one rotational) has been implemented in MATLAB. The pertinent Frequency Response Function (FRF) , $\mathbf{H}(2\pi f)$, is given by

$$\mathbf{H}(2\pi f) = (\tilde{\mathbf{K}} - (2\pi f)^2 \mathbf{M})^{-1} \boldsymbol{\tau} \quad (1)$$

where $\tilde{\mathbf{K}} = (1 + \eta i)\mathbf{K}$ is the complex stiffness matrix [17], η is the loss factor, i is the imaginary unit, \mathbf{K} and \mathbf{M} are the stiffness and mass matrices, respectively. In Equation (1) $\boldsymbol{\tau}$ is the influence vector with all the elements equal to zero, except the one corresponding to the point of modal hammer hitting that is set equal to 1:

$$\boldsymbol{\tau} = [0 \dots 0 \ 1 \ 0 \dots \dots 0]^T \quad (2)$$

It is noted that alternative damping mechanisms, e.g. viscous damping, can be clearly used for the structural identification. The hysteretic damping has been selected for its simplicity and general good accuracy avoiding a modal analysis at each iteration step that would otherwise be required for a viscous damping model, therefore reducing the computational effort. The dynamic properties were found by minimizing the difference $\boldsymbol{\varepsilon}_i(f) = |\mathbf{H}_i^{numerical}(f)| - |\mathbf{H}_i^{measured}(f)|$ between the measured and numerically evaluated FRFs at the selected three points. Specifically, the objective function J to be minimized is given by the following equation:

$$J = \boldsymbol{\varepsilon} \boldsymbol{\varepsilon}^T \quad (3)$$

where $\boldsymbol{\varepsilon} = [\boldsymbol{\varepsilon}_1(k\Delta f); \boldsymbol{\varepsilon}_2(k\Delta f); \boldsymbol{\varepsilon}_3(k\Delta f)]^T$ ($k=1\dots n$) is the $3n \times 1$ vector listing the n values of the FRFs differences discretized at Δf intervals. The minimization of Equation (3) will provide the optimal mechanical parameters for the numerical model to match the experimental results. In this paper the mass and the dimensions of the beams were assumed to be constant, as their variability has been found negligible in comparison to the mechanical properties [2], while the modulus of elasticity and the loss factors were the two parameters to be optimized.

3 Results

Beams with compressive strength of 47.25 and 63.63MPa were tested in the environmental chamber. The tests were conducted with ambient relative humidities between 58% and 69% and temperature gradually increased from -20°C to +40°C. The average temperatures measured inside the beams using the three thermocouples, were 0°C, 10°C, 20°C, and 30°C , during modal hammer tests.

Figures 5 and 6 show the trajectories of the measured relative humidity and temperature measured in the environmental chamber during the tests for both beams. From Figures 5 and 6 it can be observed that for both ambient temperature and humidity, the exposure time and pertinent fluctuations were very similar for the two different beams. However, a small shift can be observed due to the different time necessary for the two beams to reach the target internal temperature measured by the

thermocouple, showing that the beam with higher compressive strength required more time to reach the target values.

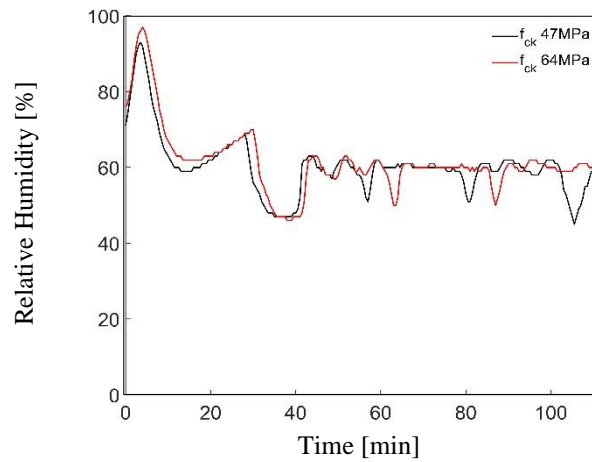


Figure 5: The variation of relative humidity in the Environmental Chamber.

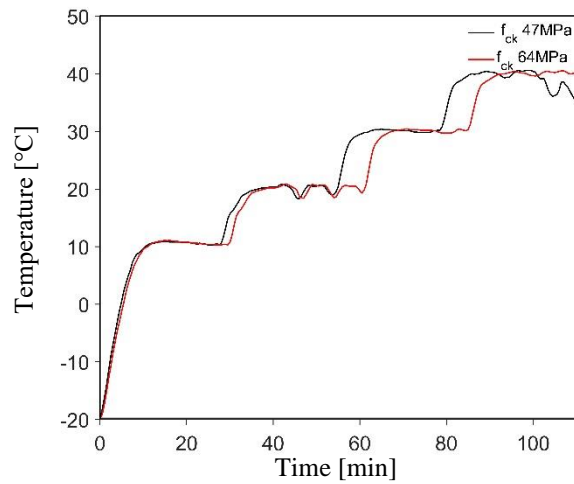


Figure 6: The variation of temperature in the Environmental Chamber.

Moreover, it has been observed during the tests, herein omitted for brevity, that different paths might lead to different results due to thermal hysteresis. Phenomenon that has been already observed at temperatures below 0°C and at elevated temperatures by other authors [18][19]. The FRFs of the experimental results revealed a shift in natural frequencies of the beam 1 (compressive strength of 47.25MPa) as a consequence of changes in the beam temperature.

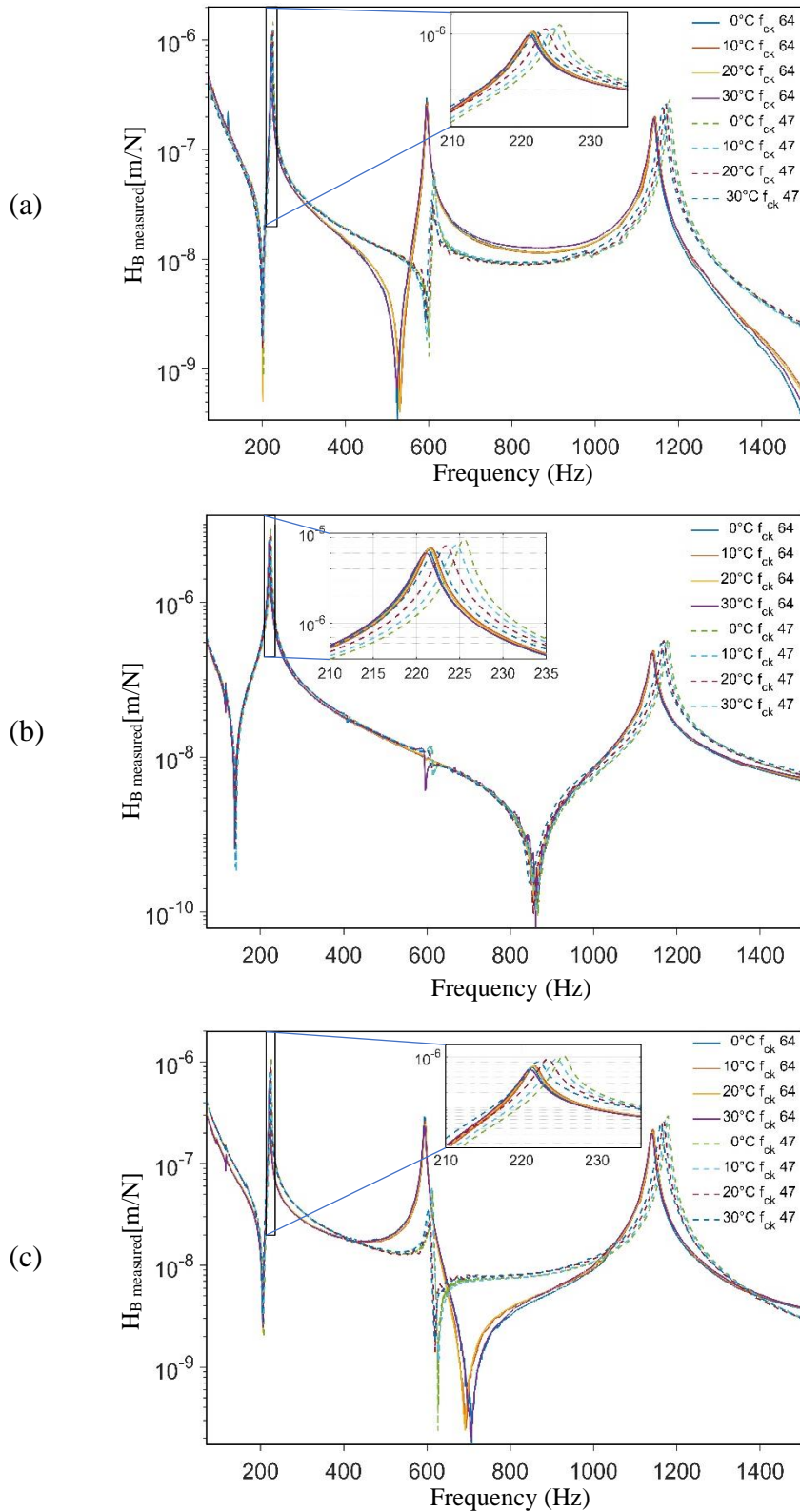


Figure 7: The measured displacement response of the three points A (a), B (b), and C (c) of the beams with compressive strengths of 64MPa and 47MPa in different temperatures

Figure 7 clearly shows that the first three bending natural frequencies of the beams are affected by changes in temperature, while the dependency of the natural frequencies of the bending modes on the temperature appears to be higher in the lower strength beam.

In addition, as shown in Figure 8, in beam 1 (compressive strength of 47.25MPa), the rate of the sensitivity of the natural frequencies to the temperature is different for each of the first three bending modes, with 1.44% reduction for the first natural frequency from temperature 0°C to 30°C, and 1.79% and 1.42% reduction for the second and third modes, respectively, within the same temperature range. While this difference is present in the first two modes of the beam 2 as well, the percentage of reduction is much lower than that of beam 1, with 0.11 and 0.084% for the first and second modes, respectively.

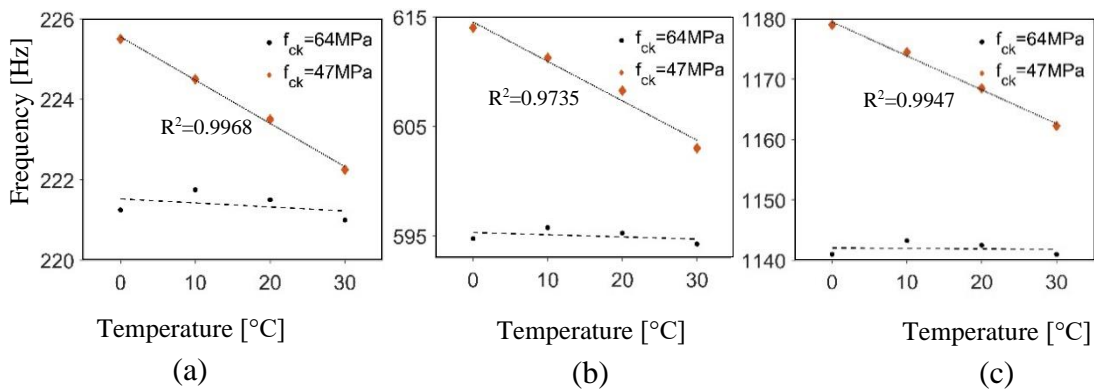


Figure 8: Temperature VS. Natural frequencies, a) First natural frequency, b) Second natural frequency, and c) Third natural frequency.

Based on the linear regression of experimental data, the trendline equation can be written as:

$$f = \beta_t T + \beta_0 \quad (4)$$

Trendline coefficients of this study are compared with the results proposed in Xia, et al. [2].

| Bending Mode | β_t (Hz/°C) | | |
|--------------|--------------------------------|--------------------------------|--------------------------------|
| | Environmental Chamber | | In-situ [2] |
| | Compressive strength 47.25 MPa | Compressive strength 63.63 MPa | Compressive strength 40.20 MPa |
| 1 | -0.1075 | -0.0100 | -0.0450 |
| 2 | -0.36 | -0.0200 | -0.0618 |
| 3 | -0.5625 | -0.0075 | -0.4974 |

Table 3: the slope coefficient of the linear regression (temperature vs. frequency).

As expected, there are some discrepancies, but the overall trend seems in line with previous studies [2][20][21][22].

The optimization algorithm was then used to identify the mechanical properties, i.e. modulus of elasticity and loss factor, of the best fitted beam numerical model. Figure 9 shows the FRFs of the results from the optimized numerical models and the equivalent experimental ones measured at points A, B and C, for a selected average internal temperature of the beam at 20°C.

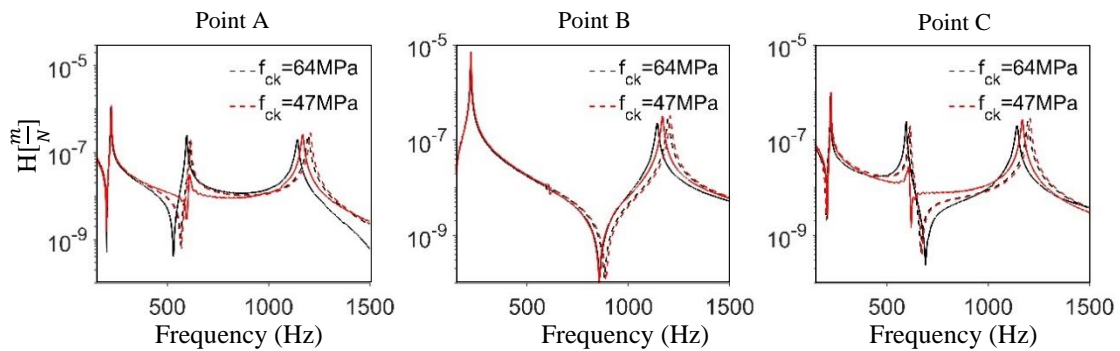


Figure 9: Numerical and experimental displacement FRFs of the two beams.

From Figure 9, it can be observed that while the first peak is captured fairly accurately from the model, there are evident discrepancies for higher modes. More advanced numerical models might be able to capture also the higher peaks with a clear cost in computational effort.

As can be seen in Figure 10, the modulus of elasticity of the concrete beam 1 has decreased by 3.02% when the temperature increased from 0°C to 30°C, while this percentage for beam 2 is only 0.17%.

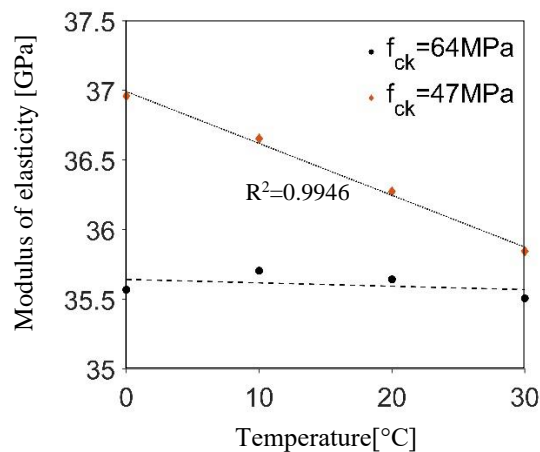


Figure 10: Identified modulus of elasticity vs temperature for the two beams with different compressive strength.

An inverse trend could be identified in terms of the changes in loss factor due to temperature variation. As shown in Figure 11, for beam with lower strength there is an increase of 28.13%, when the temperature increased from 0°C to 30°C. For the beam with higher strength the trend is less clear, with 7.07% increase in the loss factor when the temperature increased from 0°C to 30°C.

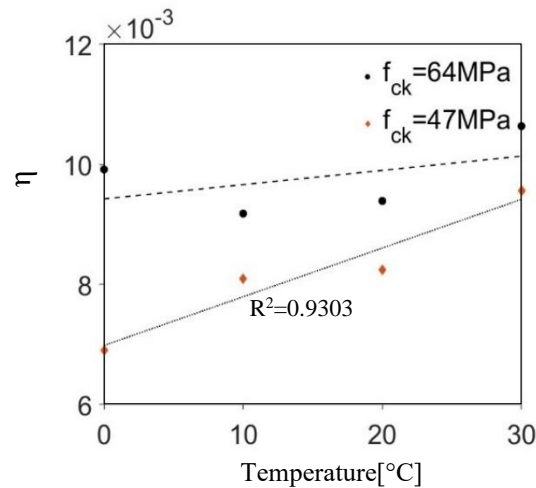


Figure11: Identified loss factor vs temperature for the two beams with different compressive strength.

4 Conclusions and Contributions

In this study, a rigorous experimental campaign was conducted in an environmental chamber to investigate the effect of temperature on natural frequencies and identified mechanical properties of two concrete beams with two different mix designs, and hence two different compressive strengths.

For each beam four modal hammer tests were done under 0°C, 10°C, 20°C, and 30°C average internal temperature, while the relative humidity of the chamber was kept in the range of 58 and 69%. The results of these tests were used to extract the first three natural frequencies, the dynamic modulus of elasticity, and the loss factor of the equivalent numerical model.

Based on the results, it was found that an increase in temperature led to a linear reduction of the values of the natural frequencies. However, it seems that the rate of this reduction is affected by the strength of the concrete specimen. Similar trend was observed in the identified modulus of elasticity.

Conversely, a positive relationship was captured between the loss factor and the temperature of the concrete beams. Again, the slope of this change seems dependent on the strength of the concrete specimen.

Obviously, more exploration is needed to confirm the linearity of these correlations, as well as the effect of mix design on the sensitivity to the hygrothermal actions.

References

- [1] R.D. Adams, P. Cawley, C.J. Pye, B. J. Stone, W.G.R Davies, "A vibration technique for non-destructively assessing the integrity of structures", *J. Mech. Eng. Sci.*, 21(1), 57, 1978.
- [2] Y. Xia, H. Hao, G. Zanardo, A. Deeks, "Long term vibration monitoring of an RC slab: temperature and humidity effect", *Engineering Structures*, 28(3), 441-452, 2006.
- [3] Y. Ding, A. Li, "Temperature-induced variations of measured modal frequencies of steel box girder for a long-span suspension bridge", *International Journal of Steel Structures*, 11, 145-155, 2011.
- [4] J. A. Ramírez, R. L. Boroschek, R. Aguilar, C. E. Ventura, "Daily and seasonal effects of environmental temperature and humidity on the modal properties of structures", *Bulletin of Earthquake Engineering*, 20(9), 4533-4559, 2022.
- [5] K. V. Yuen, S. C. Kuok, "Ambient interference in long-term monitoring of buildings. *Engineering Structures*", 32(8), 2379-2386, 2010.
- [6] C. Liu, J. T. De Wolf, "Effect of temperature on modal variability of a curved concrete bridge under ambient loads", *Journal of Structural Engineering*, 133(12), 1742-1751, 2007.
- [7] B. Peeters, G. De Roeck, "One-year monitoring of the Z24-Bridge: environmental effects versus damage events", *Earthquake engineering & structural dynamics*, 30(2), 149-171, 2001.
- [8] E. Balmes, M. Basseville, F. Bourquin, L. Mevel, H. Nasser, F. Treysede, "Merging sensor data from multiple temperature scenarios for vibration monitoring of civil structures ", *Structural Health Monitoring* 7,129-142, 2008.
- [9] M. S. Bonney, D. Wagg, "Temperature Variation Modelling of an Assembled Three-Storey Structure", *Dynamics of Civil Structures*, "Proceedings of the 40th IMAC, Volume 2", 23-31, 2022.
- [10] N. Martins, E. Caetano, S. Diord, F. Magalhães, Á. Cunha, "Dynamic monitoring of a stadium suspension roof: Wind and temperature influence on modal parameters and structural response", *Engineering Structures*, 59, 80-94, 2014.
- [11] E. J. Cross, K. Y. Koo, J. M. W. Brownjohn, K. Worden, "Long-term monitoring and data analysis of the Tamar Bridge", *Mechanical Systems and Signal Processing*, 35(1-2), 16-34, 2013.
- [12] S. Podestà, G. Riotto, F. Marazzi, "Reliability of dynamic identification techniques connected to structural monitoring of monumental buildings", *Structural Control and Health Monitoring: The Official Journal of the International Association for Structural Control and Monitoring and of the European Association for the Control of Structures*, 15(4), 622-641, 2008.

- [13] E. Shahabpoor, A. Pavic, V. Racic, S. Zivanovic, "Effect of group walking traffic on dynamic properties of pedestrian structures", *Journal of Sound and Vibration*, 387, 207-225, 2017.
- [14] Y. Xia, B. Chen, S. Weng, Y. Q. Ni, Y. L. Xu, "Temperature effect on vibration properties of civil structures: a literature review and case studies", *Journal of civil structural health monitoring*, 2, 29-46, 2012.
- [15] Standard, B. S. (1881), Method for determination of compressive strength of concrete cubes concrete specimens. BS, 116, 1983.
- [16] D. J. Ewins, "Modal testing: theory, practice and application", John Wiley & Sons, 2000.
- [17] P. Cacciola, A. Tombari, "Vibrating barrier: a novel device for the passive control of structures under ground motion", "Proceedings of the Royal Society A: Mathematical, Physical and Engineering Sciences", 471(2179), 20150075, 2015.
- [18] A. Bekele, N. Ryden, A. Gudmarsson, B. Birgisson, "Effect of cyclic low temperature conditioning on stiffness modulus of asphalt concrete based on non-contact resonance testing method", *Construction and Building Materials*, 225, 502-509, 2019.
- [19] O. Bahr, P. Schaumann, B. Bollen, J. Bracke, "Young's modulus and Poisson's ratio of concrete at high temperatures: Experimental investigations", *Materials & Design*, 45, 421-429, 2013.
- [20] H. Liu, X. Wang, Y. Jiao, "Effect of temperature variation on modal frequency of reinforced concrete slab and beam in cold regions", *Shock and vibration*, 2016.
- [21] W. Shan, X. Wang, Y. Jiao, "Modelling of temperature effect on modal frequency of concrete beam based on field monitoring data", *Shock and Vibration*, 2018, 1-13, 2018.
- [22] Z. Wang, M. Huang, J. Gu, "Temperature effects on vibration-based damage detection of a reinforced concrete slab", *Applied Sciences*, 10(8), 2869, 2020.